Energy Proceedings
Vol 57, 2025
ISSN 2004-2965

Energy-Optimized Adsorption-Liquefaction CO_2 Capture for Industrial Low-Carbon Transition

Yong Wang[1], Qiang Li[1], Yue Pang[1], Liyun Zhu[1], Zhenbo Wang [1*]

1 College of New Energy, China University of Petroleum (East China), Qingdao 266580, China

(*Corresponding Author: wangzhb@upc.edu.cn)

ABSTRACT

Optimization of integrated carbon capture processes is considered essential for addressing the challenges of low capture efficiency and high costs associated with low-concentration CO_2 streams, thereby advancing low-carbon industrial practices. In this context, an adsorption-coupled cryogenic liquefaction process is proposed. Process efficiency and system energy consumption under diverse feed conditions were systematically evaluated via simulation. Techno-economic assessment was performed considering the trade-off between capture performance and energy requirements. Simulation results indicate that at feed CO_2 concentrations of 5–15%, capture rates of 80.60–81.50% were achieved with product purity of 98.60–98.94%, while energy consumption ranged from 4.012 to 4.494 GJ/tCO_2. When optimizing for a 90% capture rate, product purity increased by 0.1% on average, though a 7.34% average increase in energy consumption was observed. Integration of this process with recoverable cold energy from gas-fired power plants could reduce energy consumption by >2 GJ/tCO_2, significantly lowering operational demands. This approach provides a validated pathway toward decarbonizing industrial systems, demonstrating both theoretical and practical significance for achieving carbon neutrality.

Keywords: Carbon capture, Process optimization, adsorption, cryogenic liquefaction process

NONMENCLATURE

Abbreviations

MOF	Metal–organic Frameworks
VTSA	Vacuum Temperature Swing Adsorption
CCUS	Carbon Capture, Utilization and Storage

Symbols

T	Temperature
P	pressure
Q	volumetric flow rate
C	Capture rate
E_C	Compression energy
E_L	Liquefaction energy
E_{TL}	Specific liquefaction energy
E_R	Regenerative energy consumption
E_T	Unit total energy consumption
E_{TA}	Unit energy consumption in adsorption

1. INTRODUCTION

Global climate change has emerged as one of the most severe challenges confronting human society. The increase in greenhouse gas emissions, particularly carbon dioxide emissions, is widely considered a primary driver of global warming[1-3]. To mitigate carbon emissions, various CCUS technologies are being continuously developed.

Current mainstream carbon capture technologies encompass chemical absorption, physical adsorption, membrane separation, and cryogenic condensation[2,5]. Among these, adsorption-based methods attract significant attention due to their high capture efficiency, operational adaptability, and regeneration feasibility, while cryogenic approaches demonstrate advantages in achieving high-purity CO_2 recovery, integration potential, and environmental compatibility. Adsorption processes primarily employ solid porous materials such as zeolites, activated carbon, or MOFs[7], selectively capturing CO_2 through physi/chemisorption mechanisms[8,9]. Plaza et al.[10] developed a non-isothermal, non-adiabatic thermodynamic model for vacuum temperature swing adsorption (VTSA) cycles, incorporating competitive gas adsorption behavior. Li et al. [11] established a

This is a paper for International CCUS Conference 2025 (ICCUSC 2025), May 28-29, 2025, Beijing, China.

mathematical modeling roadmap for adsorption-based carbon capture, identifying optimized dimensionless parameters that maximize fixed-bed utilization efficiency. At the same time, cryogenic methods exploit CO_2 condensation characteristics by implementing sub-ambient cooling to separate CO_2 from gas mixtures [12,13]. Asgharian et al. [14] systematically reviewed modeling methodologies for cryogenic carbon capture, emphasizing the necessity of integrating thermodynamic modeling, equipment-level energy simulation, and system integration optimization to accurately predict energy consumption and separation efficiency. Babar et al. [15] conducted systematic optimization analyses of temperature modulation strategies under varying pressure conditions for natural gas decarbonization, offering critical guidance for scenario-specific process design.

Distinct sub-processes—cryogenic condensation, adsorption, and compression—serve complementary functional roles within the integrated energy framework. Joint optimization of these units enables substantial reductions in specific energy consumption [16–18]. Recent advances in hybrid carbon capture systems demonstrate significant progress for gas treatment, where adsorption-coupled cryogenic processes have been strategically designed to overcome inherent limitations of single-technology approaches. Ko et al. [19] experimentally validated that such integrated adsorption-cryogenic technology achieves CO_2 capture efficiencies exceeding 90% while concurrently reducing energy intensity per tonne of CO_2 captured. Complementary energy assessments by Song et al. [20] revealed that cryogenic-adsorption hybrid pathways maintain net lower heating value efficiency within economically viable thresholds, particularly advantageous for mid-low concentration CO_2 flue gas streams. Furthermore, Maniarasu et al. [21] highlighted the superior energy performance metrics of hybrid adsorption-cryogenic systems alongside inherent benefits in modular equipment design and operational stability. Nevertheless, process tailoring for ultra-low CO_2 concentration sources demands further optimization.

This study addresses the aforementioned challenges by designing an adsorption-coupled cryogenic process through rigorous process simulation. Systematic simulations were conducted for low-concentration CO_2 flue gases (5%, 10%, and 15% vol), with process configurations optimized using the Analytic Hierarchy Process methodology. Key operational parameters governing adsorption and cryogenic liquefaction modules were investigated to quantify their impacts on CO_2 capture efficiency and specific energy consumption per unit CO_2 captured. Process optimization targeting a 90% CO_2 capture rate was implemented, demonstrating significant energy reduction while providing insights for scaling advanced hybrid carbon capture systems.

2. PROCESS FLOW MODELING

2.1 Process Parameters

The initial flue gas conditions are summarized in Tables 1 and 2.

Table 1 Flue Gas Parameters

T/℃	P/MPa	V/(Nm^3/h)
88	0.101	200

Table 2 Composition and Flow Rate of Flue Gas

component	CO_2	N_2	O_2	H_2O
Volume flow rate/(Nm^3/h)	10	150	20	20
Volume fraction /%	5	75	10	10

2.2 Process Flow Description

2.2.1 Adsorption Separation Module

The fixed bed adsorber is operated at an adsorption temperature of 75°C and atmospheric pressure, with regeneration conducted using 110°C steam. Fig. 1 depicts the schematic diagram of the adsorption separation module. During the adsorption stage, the raw flue gas stream (F1) is cooled in the heat exchanger, fed into the fixed bed adsorber, where CO_2 is adsorbed, and the treated tail gas (P1) is discharged from the top outlet. During the regeneration stage, steam (F2) is introduced into the bed; the resulting product gas stream (P2), primarily comprising CO_2 and steam, is conveyed collectively to the cryogenic separation unit.

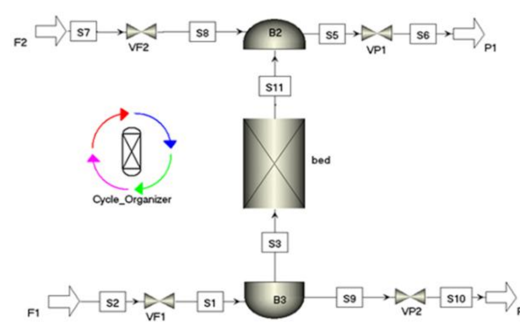

Fig. 1. Schematic Diagram of Adsorption Separation

2.2.2 Cryogenic Liquefaction Module

Fig. 2 illustrates the schematic diagram of the cryogenic liquefaction unit. The product gas stream (P2)

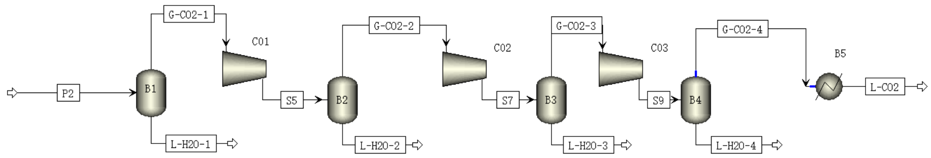

Fig. 2. Schematic Diagram of the Cryogenic Liquefaction Unit

is condensed in the Flash Drum (B1) to separate the bulk water content. The resulting vapor phase (G-CO2-1) is compressed in a three-stage compressor system. Flash drums are incorporated between compression stages to enable subsequent water condensation/separation and to reduce compressor energy consumption. The stream (G-CO2-4) is condensed to a specified temperature to yield liquid CO_2 at a pressure of 1.5 MPa.

3. PROCESS FLOW CALCULATION AND OPTIMIZATION

3.1 Computational Analysis

Fig. 3 presents the key process parameter data for the main material streams. In the diagram, F1 is designated as the raw gas feed stream, P1 is labeled as the adsorption tail gas stream, F2 is identified as the regeneration gas stream, P2 is denoted as the product gas stream, and L-CO2 is indicated as the liquid CO_2 product stream.

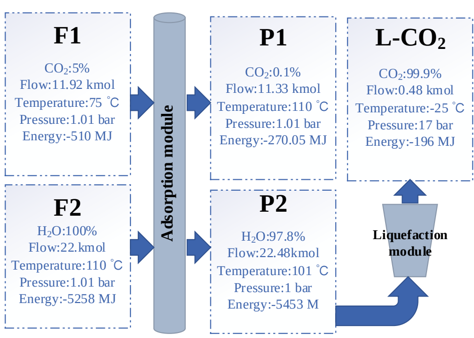

Fig. 3. Process Stream Parameters

Table 3 Results of Cryogenic Liquefaction Unit

P /bar	T /°C	H /%	C /%	E_C /MJ	E_L /MJ	E_{TL} /(GJ/tCO_2)
15	-28	99.925	99.97	7.777	62.009	3.322
17	-25	99.925	99.97	8.134	62.214	3.349
20	-20	99.924	99.97	8.610	62.439	3.382
25	-12	99.924	99.97	9.247	62.666	3.423

Table 4 Performance Indicators of the Integrated Adsorption Separation and Cryogenic Liquefaction System

η /%	C /%	E_L /MJ	E_R /MJ	E_C /MJ	E_{TL} /MJ	E_T /(GJ/tCO_2)
80	99.9	4.69	197	8.13	62.21	12.97

The cooling duties comprise precooling prior to compression (29.47 MJ), inter-stage cooling (25.95 MJ), and final liquefaction cooling (6.8 MJ). The specific energy consumption of the adsorption unit is determined to be 9.62 GJ/tCO_2, while that of the cryogenic liquefaction unit is quantified at 3.349 GJ/tCO_2. Calculation results indicate that the energy consumption of the adsorption unit is excessive, necessitating process optimization targeting adsorption temperature, adsorption duration, and desorption method.

3.2 Optimization Analysis

3.2.1 Effect of Temperature

Fig. 4 reveals that within a specific temperature range, the breakthrough point of the adsorption curve is shifted rightward and the adsorption capacity is increased with rising temperature, with the maximum adsorption capacity observed at 75 °C; further increases in temperature result in a decline in adsorption capacity.

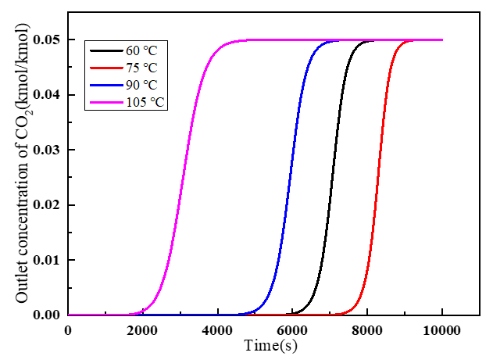

Fig. 4. Effect of Adsorption Temperature on

Fig. 5 presents the variations in product purity and exhaust gas outlet concentration versus adsorption time during the adsorption process. At 7000 s, the adsorption mass transfer zone was established to have reached the top of the bed, signifying bed breakthrough; at this point, the CO_2 concentration in the exhaust gas outlet was measured at 0.1% of the feed gas CO_2 concentration. With increasing adsorption time, enhanced bed utilization was achieved and product gas purity was observed to increase. However, the CO_2 concentration in the exhaust gas outlet concurrently increased. Consequently, excessive adsorption time will result in complete saturation of the bed with CO_2. Under this condition, CO_2 failure to be captured will occur, leading to its outflow from the bed and a reduction in capture efficiency. Through comprehensive consideration of the relationship between product purity and exhaust gas outlet CO_2 concentration, the adsorption time was determined to be 7750 s. At this specific time point, the CO_2 concentration in the exhaust gas outlet was recorded as 0.0025, equating to 5% of t he feed gas CO_2 concentration.

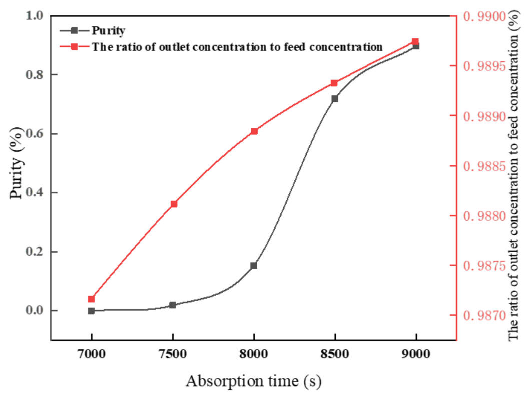

Fig. 5. Temporal Evolution of Product Purity and Effluent Concentration

3.2.3 Optimization of Regeneration Process

Analysis of Fig. 6 and Fig. 7, depicting the impact of variations in adsorption heat, adsorbent loading, and adsorption-desorption temperature difference on regeneration energy consumption, indicates that regeneration energy consumption increases with both the adsorption-desorption temperature difference and the adsorption heat, but decreases with increased adsorbent loading. Regeneration energy consumption is most significantly affected by the adsorption heat, a consequence of the high heat released during CO_2 adsorption, resulting in the desorption energy requirement constituting a major proportion of the total regeneration energy.

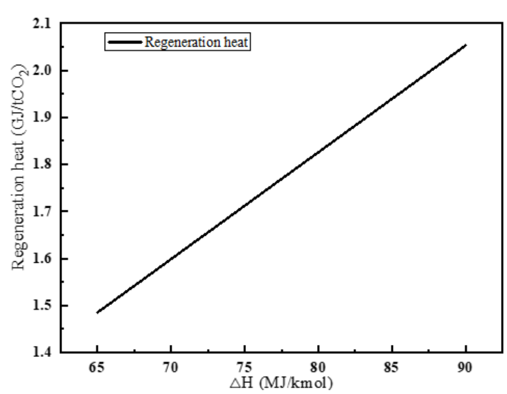

Fig. 6. Dependence of regeneration energy consumption on adsorption enthalpy variation

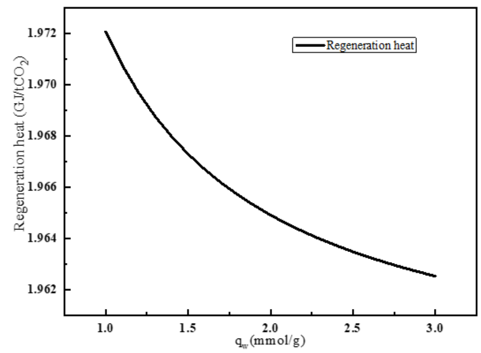

Fig. 7. Impact of adsorbent loading capacity on regeneration energy consumption

As can be observed in Fig. 8, within the range where the capture rate is 65% or higher, the regeneration energy consumption increases progressively with increasing capture rate.

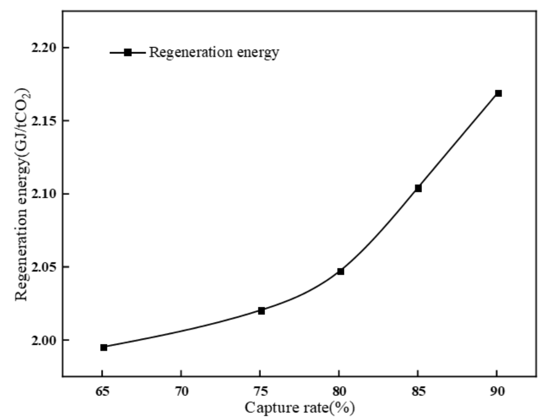

Fig. 8. Correlation Between Regeneration Energy Intensity and CO_2 Capture Efficiency

3.3 Optimization of Energy Consumption Calculation

3.3.1 5% CO_2 in Inlet Flue Gas

Analysis of Fig. 9 and 10, illustrating the influence of liquefaction temperature on CO_2 capture rate, CO_2 purity, and liquefaction unit energy consumption, reveals the following relationships: Increasing pressure was observed to broaden the range of temperatures suitable for CO_2 liquefaction and elevate the initial liquefaction temperature, while the CO_2 capture rate and purity remained largely unaffected. An increase in pressure leads to an increased compressor workload and an elevated energy consumption per unit mass. Lower temperatures are associated with an elevated overall cooling duty.

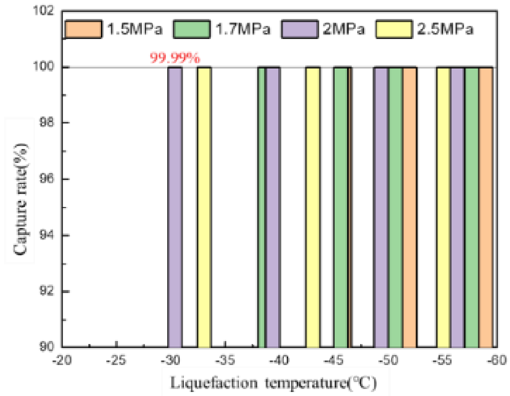

(a) Capture Rate

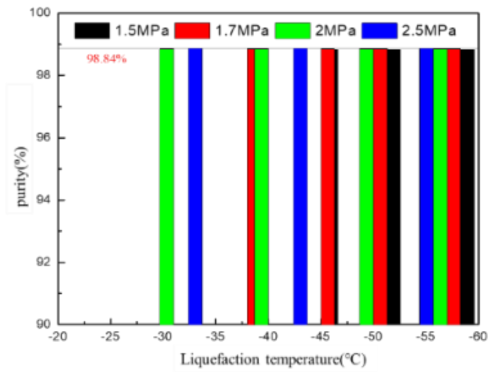

(b) Purity

Fig. 9. Cryogenic Temperature Dependence of CO_2 Capture Rate and Product Purity

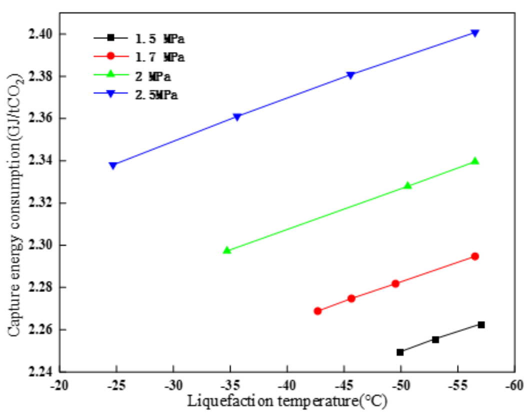

Fig. 10. Mass-Specific Energy Consumption Distribution of CO_2 Capture Rate and Product Purity

3.3.2 10% CO_2 in Inlet Flue Gas

Liquefaction of the adsorption unit's product reveals critical process interdependencies. Fig. 11 details variations in CO_2 capture efficiency, product purity, compressor duty, total refrigeration load, and mass-specific energy consumption across differential compression pressures and cryogenic temperatures. Under specified conditions, adsorbent regeneration energy dominated the energy profile at 2.05 GJ/tCO_2 (accounting for 95% of total consumption), while feedstock liquefaction energy required 0.11 GJ/tCO_2.

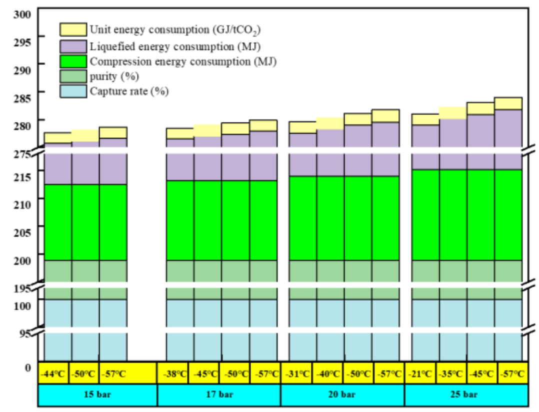

Fig. 11. Thermodynamic Performance Analysis of Cryogenic Liquefaction Unit

The influence of increasing pressure on the CO_2 liquefaction process was characterized as follows: the range of temperatures suitable for CO_2 liquefaction was broadened and the initial liquefaction temperature was elevated, while the CO_2 capture rate and purity remained largely unaffected. The capture rate was observed to be marginally higher than that achieved with flue gas containing 5% CO_2. Pressure augmentation leads to an increased compressor workload and an elevated energy consumption per unit mass. The energy consumption per unit mass for cryogenic separation was determined to range between 1.9 and 2.1 GJ/tCO_2, representing a reduction of 0.3 GJ/tCO_2 compared to the process treating 5% CO_2 flue gas.

Based on the energy consumption calculated for the adsorption-desorption section and the cryogenic liquefaction section, the overall system energy consumption was calculated. Using the cryogenic liquefaction unit operating at 15 bar and -44 °C as a representative case, the calculated results are presented in Fig. 13. The energy consumption per unit mass was found to be 2.16 GJ/tCO_2 for the adsorption unit and 1.94 GJ/tCO_2 for the cryogenic liquefaction unit.

3.3.3 15% CO_2 in Inlet Flue Gas

Fig. 12 presents the flue gas conditions corresponding to a 15% CO_2 concentration and the energy consumption profile of the adsorption unit. Liquefaction was performed on the product gas derived from the adsorption unit. Subsequently, variations in CO_2 capture rate, product purity, compressor workload, total cooling duty, and energy consumption per unit mass were calculated under different compression pressures and cryogenic temperatures.

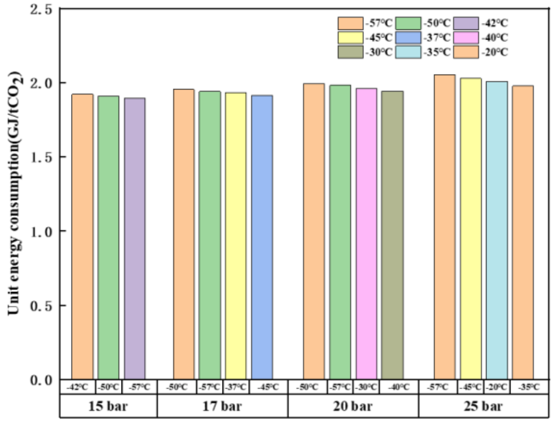

Fig. 12. Parametric Trends of Pressure and Temperature on Specific Energy Consumption

Increasing pressure was observed to broaden the range of temperatures suitable for CO_2 liquefaction and elevate the initial liquefaction temperature, while the CO_2 capture rate (99.99%) and purity (98.95%) remained essentially constant. The capture rate was found to be marginally higher than that achieved with flue gas containing 10% CO_2. An increase in pressure leads to an increased compressor workload and an elevated energy consumption per unit mass. The energy consumption per unit mass for cryogenic separation was determined to be in the range of 1.85 to 2.05 GJ/tCO_2, representing a reduction of 0.05 GJ/tCO_2 compared to the process treating 10% CO_2 flue gas.

The overall system energy consumption was calculated based on the energy consumption associated with the adsorption-desorption section and the liquefaction section. Taking the cryogenic liquefaction unit operating at 15 bar and -42 °C as an example case, the calculation results are presented in Fig. 15. The energy consumption per unit mass was calculated to be 2.12 GJ/tCO_2 for the adsorption unit and 1.89 GJ/tCO_2 for the cryogenic liquefaction unit. System energy consumption was further calculated for different CO_2 concentrations of 5%, 10%, and 15%, with the results also presented in Fig. 13.

As the CO_2 concentration in the feed increases, the overall system energy consumption decreases. This trend is attributed to the concomitant rise in the partial pressure of CO_2 within the feed gas resulting from the higher concentration. This elevated partial pressure leads to an increased saturation capacity of the adsorbent. Consequently, a greater mass of CO_2 can be adsorbed within the same adsorbent bed volume. Ultimately, the enhanced quantity of CO_2 processed by the system results in a reduction in the overall energy consumption per unit mass of CO_2 captured.

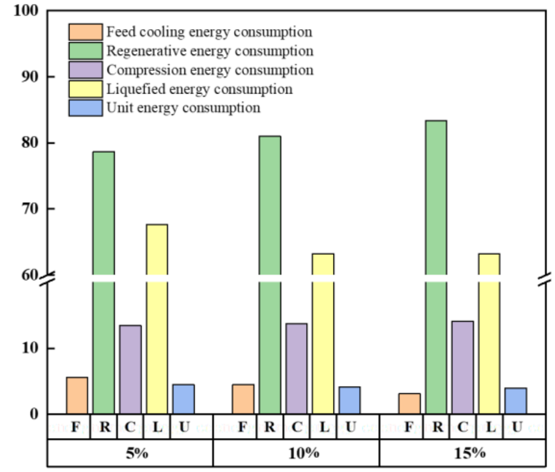

Fig. 13. Synergistic Effect of Critical P-T Thresholds on Energy Demands

3.4 Optimization of 90% CO_2 Recovery Rate

The simulation constraints were specified as a minimum purity exceeding 95% and a recovery rate greater than 80%. As indicated in Fig. 14, an increase in the desorption time was observed to correlate with a corresponding increase in both the CO_2 recovery rate and the product purity. Consequently, under constant adsorption process operating parameters, extending the regeneration time can be implemented to effectively enhance the recovery rate.

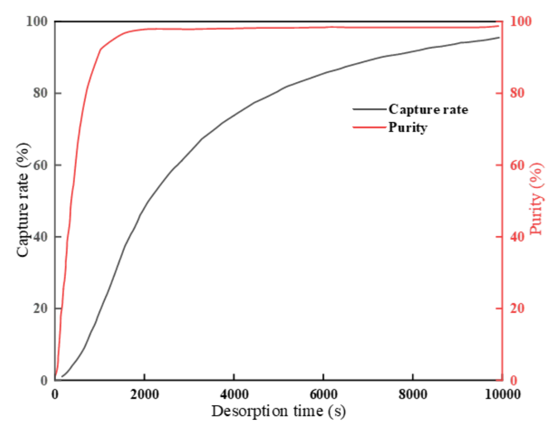

Fig. 14. Relationship Between CO_2 Recovery Rate and Product Purity

The performance metrics of the adsorption + cryogenic separation system at different feed CO_2 concentrations are presented in Fig. 15. As the CO_2 recovery rate increased to 90%, the energy consumption of both the adsorption unit and the cryogenic liquefaction unit was observed to increase, resulting in a corresponding rise in the system's specific energy consumption for capture.

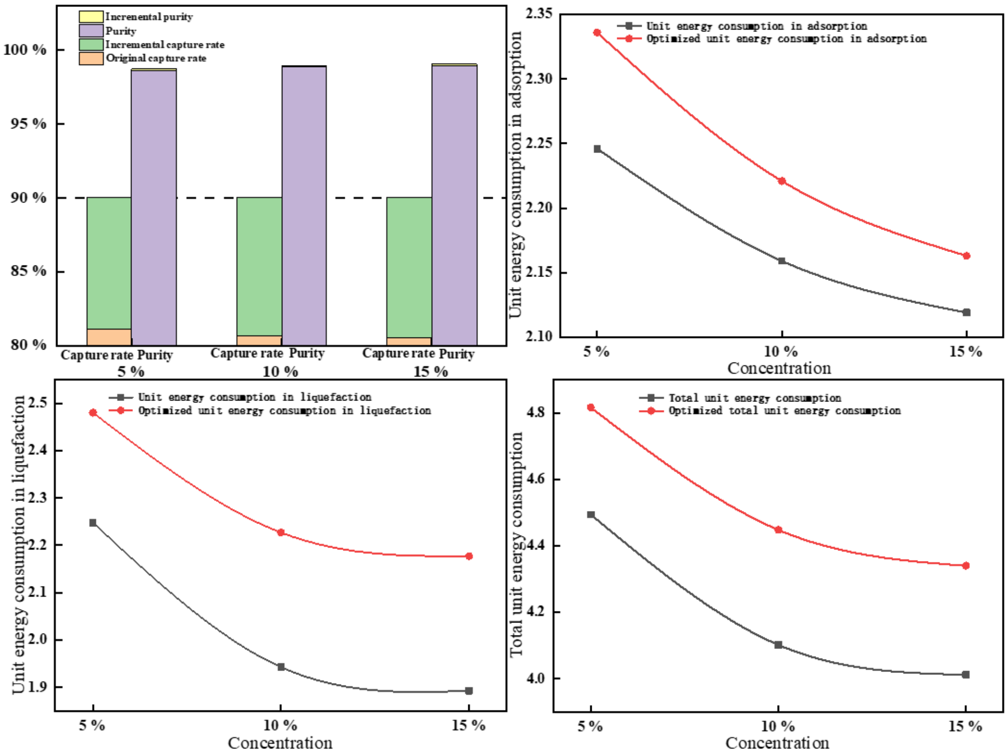

Fig. 15. Influence of CO_2 Concentration Gradients on Specific Energy Consumption Pre- and Post-Optimization

Significant variations in system-wide energy consumption and capture performance emerge under different initial CO_2 concentrations. At 5% CO_2 concentration, with the cryogenic liquefaction unit operating at baseline conditions (15 bar, -46 °C), mass-specific energy consumption reached 2.34 GJ/tCO_2 for the adsorption unit and 2.48 GJ/tCO_2 for cryogenic liquefaction, yielding total system energy consumption of 4.82 GJ/tCO_2. This configuration achieved 90% capture efficiency with 98.73% product purity. When concentration increased to 10%, cryogenic parameters were optimized to -42 °C (maintaining 15 bar), reducing adsorption energy to 2.22 GJ/tCO_2 and liquefaction energy to 2.23 GJ/tCO_2. Consequently, total energy consumption decreased to 4.45 GJ/tCO_2 while maintaining 90% capture efficiency and elevating purity to 98.95%. At 15% CO_2 concentration (cryogenic unit: -41 °C, 15 bar), adsorption energy further declined to 2.16 GJ/tCO_2 and liquefaction to 2.18 GJ/tCO_2, optimizing total consumption to 4.34 GJ/tCO_2. This regime sustained 90% capture efficiency while delivering peak purity of 99.04%. These results collectively indicate an inverse relationship between initial CO_2 concentration and total system energy consumption, coupled with simultaneous enhancement of product purity. Within the constraint of ⩾90% capture efficiency, higher feedstock CO_2 content consistently correlates with lower specific capture energy.

4. CONCLUSIONS

Carbon capture was investigated for low-concentration CO_2 flue gases, such as those from cement plants and gas-fired power plants. The influence mechanisms of different operating conditions on enhancing capture efficiency and reducing system energy consumption were examined. Utilizing process simulation software, an integrated carbon capture process was designed. Based on the Analytic Hierarchy Process, a techno-economic analysis was conducted for the integrated capture process, yielding the following conclusions:

1.An integrated adsorption-coupled cryogenic liquefaction process was designed for carbon capture, achieving simultaneous production of liquid CO_2 product and delivering enhanced capture efficiency with minimized system-wide energy consumption. This hybrid configuration demonstrates significant improvements in energy efficiency while maintaining purity of the cryogenic product.

2.Process simulation and system optimization were performed for industrial flue gases containing 5%, 10%, and 15% CO_2 concentrations. At a 5% CO_2 concentration, the system capture rate was 81.12%, the product purity was 98.60%, and the system energy consumption was 4.49 GJ/tCO_2. At a 10% CO_2 concentration, the capture rate was 80.65%, the purity was 98.84%, and the energy consumption was 4.10 GJ/tCO_2. At a 15% CO_2 concentration, the capture rate was 81.50%, the purity was 98.94%, and the energy consumption was 4.01 GJ/tCO_2.

3.To further enhance system processing capacity and increase the capture rate to 90%, the following results were obtained: At a 5% CO_2 concentration, the product purity remained at 98.60% (an increase of 1.3‰), while the system energy consumption rose to 4.82 GJ/tCO_2 (an increase of 6.69%). At a 10% CO_2 concentration, the purity remained at 98.84% (an increase of 1.1‰), and the energy consumption increased to 4.45 GJ/tCO_2 (an increase of 7.78%). At a 15% CO_2 concentration, the purity remained at 98.94% (an increase of 1.0‰), and the energy consumption rose to 4.34 GJ/tCO_2 (an increase of 7.56%).

The designed adsorption coupled four-stage separation and three-stage compression cryogenic liquefaction process demonstrates significant advantages in application scenarios with abundant redundant high-grade cold sources, such as gas-fired power plants, particularly for the efficient utilization of cryogenic methods. This process design contributes to accelerating the establishment of global climate governance systems and holds considerable theoretical and practical significance for advancing towards a zero-carbon industrial system.

ACKNOWLEDGEMENT

The research reported in this publication was supported by funding from China University Petroleum (East China).

DECLARATION OF INTEREST STATEMENT

The authors declare that they have no known competing financial interests or personal relationships that could have appeared to influence the work reported in this paper. All authors read and approved the final manuscript.

REFERENCES

[1]IEA. Global Energy Review 2025,[R]. Paris: IEA, 2025.

[2]McLaughlin H, Littlefield A A, Menefee M, et al. Carbon capture utilization and storage in review: Sociotechnical implications for a carbon reliant world[J]. RENEW SUST ENERG REV, 2023,177:113215.

[3]Haszeldine R S. Carbon Capture and Storage: How Green Can Black Be?[J]. SCIENCE, 2009,325(5948):1647-1652.

[4]Shirafkan S M, Ledari M B, Mohebbi K, et al. Revolutionising the petrochemical supply chain: Integrating waste and CO2 from CCUS into a low-carbon circular economy framework[J]. J. Environ. Chem. Eng, 2025,13(3):116722.

[5]Witte K. Social Acceptance of Carbon Capture and Storage (CCS) from Industrial Applications[J]. SUSTAINABILITY-BASEL, 2021,13(21):12278.

[6]Li B, Huang W, Li X, et al. A review of CO2 leakage along faults in CCUS: Theories, experiments, and models[J]. Gas Sci. Eng, 2025,139:205641.

[7]Karimi M, Shirzad M, Silva J A C, et al. Carbon dioxide separation and capture by adsorption: a review[J]. Environ. Chem. Lett, 2023,21(4):2041-2084.

[8]Zhao H, Luo X, Zhang H, et al. Carbon-based adsorbents for post-combustion capture: a review[J]. GREENH GASES, 2018,8(1):11-36.

[9]Chuah C Y, Ho Y L, Syed A M H, et al. Applicability of Adsorbents in Direct Air Capture (DAC): Recent Progress and Future Perspectives[J]. Ind. Eng. Chem. Res, 2025,64(8):4117-4147.

[10]Plaza M G, Durán I, Rubiera F, et al. Adsorption-based Process Modelling for Post-combustion CO2 Capture[J]. Energy Procedia, 2017,114:2353-2361.

[11]Li S, Deng S, Zhao L, et al. Mathematical modeling and numerical investigation of carbon capture by adsorption: Literature review and case study[J]. Appl. Energy, 2018,221:437-449.

[12]Berstad D, Anantharaman R, Nekså P. Low-temperature CO2 capture technologies – Applications and potential[J]. Int. J. Refrig, 2013,36(5):1403-1416.

[13]Chen P, Ceschin A, Rahantamialisoa F N Z, et al. A computational study of desublimation tower characteristics for Cryogenic Carbon Capture[J]. Appl. Therm. Eng, 2025,267:125698.

[14]Asgharian H, Iov F, Araya S S, et al. A Review on Process Modeling and Simulation of Cryogenic Carbon Capture for Post-Combustion Treatment[J]. ENERGIES, 2023,16(4):1855.

[15]Babar M, Bustam M A, Maulud A S, et al. Optimization of cryogenic carbon dioxide capture from natural gas[J]. Materialwiss. Werkstofftech, 2019,50(3):248-253.

[16]Zhao L, Primabudi E, Stolten D. Investigation of a Hybrid System for Post-Combustion Capture[J]. Energy Procedia, 2014,63:1756-1772.

[17]Oh J, Anantharaman R, Zahid U, et al. Process design of onboard membrane carbon capture and liquefaction systems for LNG-fueled ships[J]. Sep. Purif. Technol, 2022,282:120052.

[18]Kang J, Ko Y, Jung M Y, et al. Industrial-scale 12-layered-bed vacuum pressure swing adsorption for fuel

cell-grade H2 production from carbon-captured steam methane reforming syngas[J]. Chem. Eng. J, 2024,499:156068.
[19]Ko Y, Kang J, Do H, et al. Hybrid process using cryogenic and pressure swing adsorption process for CO2 capture and extra H2 production from a tail gas in a steam methane reforming plant[J]. Energy Convers. Manage, 2025,328:119561.
[20]Song C, Liu Q, Ji N, et al. Alternative pathways for efficient CO2 capture by hybrid processes—A review[J]. RENEW SUST ENERG REV, 2018,82:215-231.
[21]Murugan R M S K. A review on materials and processes for carbon dioxide separation and capture[J]. Energy Environ, 2023,34(1):3-57.